Photocatalytic production of bisabolene from green microalgae mutant: process analysis and kinetic modeling

Photocatalytic production of bisabolene from green microalgae mutant: process analysis and kinetic modelling

Irina Harun[a,ǂ], Ehecatl Antonio Del Rio-Chanona[a,b,ǂ], Jonathan L. Wagner[a,f], Kyle J. Lauersen[e], Dongda Zhang[a,b,c,d,*], Klaus Hellgardt[a,*]

[a]*Department of Chemical Engineering, Imperial College London, South Kensington, United Kingdom, SW7 2AZ*

[b]*Centre for Process Systems Engineering, Imperial College London, South Kensington Campus, London SW7 2AZ, UK*

[c]*School of Chemical Engineering and Analytical Science, The University of Manchester, Oxford Road, Manchester, M1 3BU, UK*

[d]*Centre for Process Integration, The University of Manchester, Oxford Road, Manchester, M1 3BU, UK*

[e]*Faculty of Biology, Bielefeld University, Universitätsstraße 25, 33615 Bielefeld, Germany*

[f]*Department of Chemical Engineering, University of Loughborough, Loughborough, LE11 3TU, UK*

Tel: +44 (0) 1509 222546

ǂ*: These authors contributed equally to this work.*

: corresponding authors, email: dongda.zhang@manchester.ac.uk (Dongda Zhang); k.hellgardt@imperial.ac.uk (Klaus Hellgardt).

Abstract

Currently, algal fuel research has commenced to shift towards genetically engineered mutants, able to express and excrete desired products directly into the culture. In this study, a mutant strain of *Chlamydomonas reinhardtii*, engineered for bisabolene (alternative biodiesel) excretion, was cultivated at different illumination and temperatures to investigate their effects on cell growth and bisabolene production. Moreover, a kinetic model was constructed to identify the desirable conditions for biofuel synthesis. Three original contributions were concluded. Firstly, this work confirmed that bisabolene was partially synthesised independently of biomass growth, indicating its feasibility for continuous production. Secondly, it was found that whilst bisabolene synthesis was independent of light intensity, it was strongly affected by temperature, resulting in conflicting desirable conditions for cell growth and product synthesis. Finally, through model prediction, optimal operating conditions were identified for mutant growth and bisabolene synthesis. This study therefore paves the way towards chemostat production and process scale-up.

Keywords: Photocatalysis; Kinetic modelling; Photobioreactor; Excreted biofuels; Process optimisation.

Introduction

Autotrophic organisms such as microalgae and cyanobacteria have long been regarded as highly promising feedstocks for the production of third-generation biofuels. These organisms display rapid growth rates and require minimal input of trace elements, using light to harvest CO_2 as the sole carbon source [1–4]. However, commercial progress of algae derived biofuels has been slow, limited by the high costs of algae cultivation, harvesting, and downstream processing. Current production facilities are based around the cultivation of oleaginous strains for algal lipids, which are subsequently solvent-extracted and converted into biodiesel via transesterification and hydrotreatment [5]. An alternative approach is the hydrothermal liquefaction of the whole, wet biomass-culture to produce crude bio-oils for further upgrading into fuels [6,7]. Although these technologies are relatively well established and produce fuels compatible with the existing transport infrastructure, they are inefficient and costly [8].

Consequently, engineering microalgae and cyanobacteria to excrete desired products directly into the culture medium is a highly desired solution to overcome the limitations of conventional solvent extraction concepts. Secretion, or excretion, enables straightforward and efficient recovery of a desired (fuel) product separate from the valuable algal biomass, which can be used for any number of alternative applications or recycled within the reactor. In this way, the cells effectively act as a photo-catalyst or green-cell factory, converting light, CO_2 and water into a desired product. To date, the production and excretion of a number of products has already been successfully demonstrated, including free fatty acids [9], alcohols, *e.g.* ethanol [10], isopropanol [11] or butanol, and terpenoids, such as farnasene [12], limonene [13], and patchoulol [14].

Terpenoids are particularly interesting targets for microbial photobiocatalysis as some have favourable fuel properties, but are produced in their native hosts to only low titres [15]. For example, the sesquiterpene (C15) (*E*)-α-bisabolene (hereafter bisabolene) is natively produced in the grand fir, *Abies grandis* [16], and can be hydrogenated into bisabolane, which has particularly attractive properties as a diesel-like drop-in fuel [17]. Green algae and cyanobacteria are considered to be valuable hosts for terpenoid production as their native metabolism is structured to produce terpenoid molecules by the methylerythritol phosphate pathway (MEP) from glyceraldehyde-3-phosphate (G3P) and pyruvate [18], representing ~5% of cellular carbon flux [19]. Genetically modified strains of *Synechococcus* sp. PCC 7002 were previously shown to produce bisabolene up to 0.6 mg L^{-1} after 96 h [20]. Very recently, *Chlamydomonas reinhardtii* was also engineered to produce and excrete bisabolene up to 8 mg L^{-1} in 96 h [21].

To facilitate process scale-up, it is vital to understand effects of environmental conditions on terpenoid synthesis in photobioreactors (PBRs). A PBR is an enclosed reactor system in which illumination and nutrients are provided to facilitate algae biomass growth and biorenewables synthesis. Both light and temperature are known to have strong influences on algal productivity as well as metabolic partitioning of native products. For example, commercial production of terpenoid derived pigments (*e.g. β*-carotene and astaxanthin) from green algae uses high light conditions to hyper-accumulate these photo-protective carotenoids [22]. As bisabolene is a heterologous terpenoid product for the green algal cell, it is necessary to characterise and generate kinetic models for its production optimisation. Therefore, in this paper, a mutant strain of the green microalgae, *C. reinhardtii,* genetically modified to enable the secretion of

bisabolene, are utilised to investigate the effect of light intensities and temperatures on cell growth and bisabolene production. A kinetic model was constructed for the first time to simulate the influence of these key operating conditions, with the aim to investigate the biochemical reaction mechanisms and predict the optimal operating conditions for the excreted biofuel synthesis.

Materials and methods

Microalgal strain and its preculture conditions

The experiments were conducted with a strain of *Chlamydomonas reinhardtii* UVM4 [23] genetically engineered with the bisabolene synthase gene (*Abies grandis* bisabolene synthase Uniprot: O81086). The strain was was generated from single transformation of vector ii as described in Wichmann et al. (2018) [21], and was obtained from the Kruse group at Bielefeld University. The cultures were grown in the Tris-acetate phosphate (TAP) growth medium [24], using a modified trace metal solution to yield final concentrations of 20.5 µM $FeCl_3 \cdot 6H_2O$, 2.5 µM $ZnSO_4 \cdot 7H_2O$, 2.0 µM $CuSO_4 \cdot 5H_2O$, 6.5 µM $MnCl_2 \cdot 4H_2O$, 0.2 µM $(NH_4)_6Mo_7O_{24} \cdot 4H_2O$ and 57.5 µM $Na_2EDTA \cdot 2H_2O$.

Operation of photobioreactor

Growth experiments were conducted in a 1 L vertical flat-plate bioreactor, constructed from polymethyl methacrylate, as described previously [25]. The system consists of a 1 L growth chamber, illuminated by a cool white LED array and maintained at constant temperature via a secondary heating water compartment. The employed cultivation temperatures ranged from 22 ºC to 32 ºC, with incident light intensities ranging from 20 µE to 300 µE. Temperature, pH and

light transmission probes provided constant monitoring of the culture conditions, while a sampling port at the bottom of the reactor allowed regular withdrawal of culture samples for external analysis. Mixing and the addition of atmospheric CO_2 was provided using filtered air bubbled continuously through a tubular sparger.

Analytical procedures

Growth monitoring: The system temperature was continuously monitored using the thermocouple and the water bath temperature was adjusted manually to obtain the desired cultivation temperature. Dry weight measurements of culture samples were conducted using vacuum filtration of 10 mL of culture (Millipore membrane filters, 5.0 µm small molecular weight protein), followed by drying at 60 °C to constant weight. To continuously monitor biomass growth, the light transmission probe readings were used to back-calculate biomass dry weight, after calibration with the sampled dry weight readings. The pH was obtained from the internal electrode, calibrated by three-point calibration at pH 4.0, 7.0 and 10.0.

***Measurement of bisabolene concentration*:** Bisabolene was extracted from 10 mL whole culture samples using 2 mL of dodecane. The organic phase was directly analysed on a Hewlett Packard 5890 gas chromatograph with an Agilent HP-5 column (50 m, 0.32 mm x 0.25 µm) and a flame ionisation detector (FID). 1 µL samples were injected at 250 °C in splitless mode using a nitrogen carrier gas flowrate of 1 ml min^{-1}. The initial oven temperature was 80 °C, held for 1 min, followed by ramping at 10 °C min^{-1} from 80 °C to 120 °C, 3 °C min^{-1} from 120 °C to 160 °C and again 10 °C min^{-1} from 160 °C to 270 °C, with a final hold time of 2 min.

Bisabolene concentrations were quantified using standard calibration curves for bisabolene (Alfa Aesar, bisabolene, mixture of isomers).

Model construction methodology

***Simulation of biomass growth*:** Algal biomass growth is under nutrient-sufficient conditions due to the presence of multiple carbon nutrients including acetate and CO_2.The Logistic model (Equation 1) was therefore adopted in this work as it has been widely used to simulate microorganism cell growth under such conditions for both traditional fermentation processes [26] and microalgae photo-production systems [27]. In this equation, the first term on the right denotes biomass growth rate, and the second term denotes algae decay rate.

$$\frac{dX}{dt} = \mu \cdot X \cdot \left(1 - \frac{X}{X_{\max}}\right) = \mu \cdot X - \mu_d \cdot X^2 \quad (1)$$

where X is biomass concentration, μ is biomass specific growth rate, $X_{\max}$ is maximum biomass concentration, and μ_d is biomass specific decay rate. Units of parameters are listed in Table 3.

***Simulation of light intensity and temperature effects on algal growth*:** To account for the effects of cultivation conditions on biomass growth, the biomass specific growth rate, μ, was expanded to include factors for light intensity and temperature (Equation 2a). These were estimated from the Aiba model (Equation 2b) and an Arrhenius-type equation (Equation 2c), respectively, commonly used for the modelling of green algae biomass [28]. The specific version of the Arrhenius equation was selected based on its higher accuracy compared to the other Arrhenius equation derived models derived for microorganism growth [28,29] and transformed further into Equation 2d to facilitate system identification.

$$\mu = \mu_m \cdot k(I) \cdot k(T) \quad (2a)$$

$$k(I) = \frac{I(z)}{I(z) + k_s + \frac{I(z)^2}{k_i}} \quad (2b)$$

$$k(T) = A_c \cdot \exp\left[-\frac{E_a}{RT}\right] - A_d \cdot \exp\left[-\frac{E_b}{RT}\right] \quad (2c)$$

$$k(T) = \exp\left[-\left(\frac{E_a}{RT} - \frac{E_a}{RT_a}\right)\right] - \exp\left[-\left(\frac{E_b}{RT} - \frac{E_b}{RT_b}\right)\right] \quad (2d)$$

where μ_m is maximum biomass specific growth rate, $I(z)$ is local light intensity, k_s is the photosaturation term, k_i is the photoinhibition term, A_c and A_d are pre-exponential parameters, E_a is the algae activation energy, E_b is the algae deactivation energy, T is the culture temperature, $T_a$and $T_b$are reference temperatures, and R is the gas constant.

***Simulation of light attenuation in a PBR*:** Effects of light attenuation within the PBR, caused by algae cell absorption and bubble scattering [30], were modelled by embedding the modified Lambert-Beer's law into the current kinetic model (Equation 3). To prevent the complexity of modelling the resulting partial differential equation (PDE), constituting both spatial and temporal dimensions which limits the model's further applicability to real-time dynamic optimisation in fed-batch and continuous processes, a 10-step Trapezoidal rule was applied to eliminate the spatial dimension (Equation 4).

$$I(z) = I_0 \cdot \exp[-(\tau \cdot X + K_a) \cdot z] \quad (3)$$

$$k(I) = \frac{1}{20} \cdot \sum_{n=1}^{9} \left(\frac{I_{i=0}}{I_{i=0} + k_s + \frac{I_{i=0}^2}{k_i}} + 2 \cdot \frac{I_{i=\frac{n \cdot L}{10}}}{I_{i=\frac{n \cdot L}{10}} + k_s + \frac{I_{i=\frac{n \cdot L}{10}}^2}{k_i}} + \frac{I_{i=L}}{I_{i=L} + k_s + \frac{I_{i=L}^2}{k_i}} \right) \quad (4)$$

where I_0 is incident light intensity, τ is algal cell absorption coefficient, K_a is the bubble scattering coefficient, z is the distance from light source, L is the width of the PBR, and I_i is the local light intensity at a distance of $i = \frac{n \cdot L}{10}$ from the PBR front exposure surface.

***Simulation of bisabolene production*:** To simulate bisabolene synthesis, the Luedeking–Piret model is applied and modified in this work [31]. The original Luedeking–Piret model is presented in Equation 5a, where the first term on the right denotes the cell growth related bisabolene production and the second term represents the growth independent bisabolene production. Despite the original model being able to capture the kinetics of most bacterial fermentation processes, it assumes that effects of light intensity and temperature on bioproducts synthesis are equal to those on microalgae biomass growth, Nonetheless, for most of the currently explored algal bioproducts *e.g.* hydrogen, astaxanthin and phycocyanin, previous studies have declared that optimal operating conditions for these bioproducts synthesis are different or even conflicting from those for algae cell growth [32–34]. Therefore, to accurately simulate bisabolene production, the original Luedeking–Piret model is modified to Equation 5b based on the current experimental observation and analysis. The detailed explanation for this modification is presented in the Results and Discussion section.

$$\frac{dP}{dt} = Y_1 \cdot \frac{dX}{dt} + Y_2 \cdot X \qquad (5a)$$

$$\frac{dP}{dt} = \left(Y_1 \cdot \frac{dX}{dt} + Y_2 \cdot X\right) \cdot \left(\alpha - \left(\exp\left[-\left(\frac{E_a}{RT} - \frac{E_a}{RT_a}\right)\right] - \exp\left[-\left(\frac{E_b}{RT} - \frac{E_b}{RT_b}\right)\right]\right)\right) \qquad (5b)$$

where P is bisabolene production, Y_1 is biomass growth associated bisabolene yield coefficient, Y_2 is biomass growth independent bisabolene yield coefficient, and α is a temperature related dimensionless modification parameter for bisabolene synthesis rate.

***Experimental data selection*:** To guarantee the high accuracy and predictive capability of the current model, four sets of experimental data were used for dynamic model parameter estimation, with another four datasets obtained from experiments operated at conditions different from the previous four experiments used for model verification (Table 1).

Table 1: Operating conditions of experiments for parameter estimation and model prediction

Experiments for model fitting (parameter estimation)				
	Experiment 1	Experiment 2	Experiment 3	Experiment 4
Light intensity	20 µE m^{-2} s^{-1}	300 µE m^{-2} s^{-1}	60 µE m^{-2} s^{-1}	60 µE m^{-2} s^{-1}
Temperature	30 ºC	30 ºC	26 ºC	32 ºC
Experiments for model predictive capability verification				
	Test 1	Test 2	Test 3	Test 4
Light intensity	40 µE m^{-2} s^{-1}	100 µE m^{-2} s^{-1}	60 µE m^{-2} s^{-1}	60 µE m^{-2} s^{-1}
Temperature	30 ºC	30 ºC	28 ºC	22 ˚ ºC

Parameter estimation methodology

An accurate parameter estimation framework is crucial to guarantee the accuracy and predictive power of the developed dynamic model. Given the high accuracy of measurement instruments and the assumption that measurement noise follows a normal distribution, a weighted nonlinear least squares optimisation problem is formulated to determine the optimal set of parameters that identify the system. Because of the nonlinearity and stiffness of the DAE model, stiff system integration methods are required, and hence orthogonal collocation over finite elements in time using Radau roots was used [35]. This method has proven to be highly

efficient for discretising dynamic systems, and computational costs are reduced significantly compared to simpler discretisation schemes (*e.g.* implicit Euler method) [36]. The parameter estimation problem in an orthogonal collocation formulation is presented in Equations 6a-h.

$$\min_{p,x} \sum_{i=1}^{N} \left(\hat{x}_i - x(t_i,p)\right)^T \alpha_i \left(\hat{x}_i - x(t_i,p)\right) \quad (6a)$$

subject to:

process dynamics

$$\dot{x}_{i,j} = f\left(x_{i,j}, \dot{x}_{i,j}, p\right) \quad (6b)$$

collocation constraints

$$x_{i,j} = x_{i-1,K} + h_i \sum_{l=1}^{K} \varphi_l(\tau_j)\, \dot{x}_{i,l} \quad (6c)$$

continuity constraints

$$x_{i,0} = x_{i-1,K} \quad (6d)$$

initial conditions

$$x_{1,0}(t_0) = x_0 \quad (6e)$$

integration horizon

$$0 \le t \le t_f \quad (6f)$$

bounds

$$x_{lb} \le x \le x_{ub} \quad (6g)$$

$$p_{lb} \le p \le p_{ub} \quad (6h)$$

where x is the vector of variables containing the chemicals and algal species in the model, $\hat{x}$ is the measured states, p is the vector of the model parameters to be determined, α is the

weighting factor, and *N* is the number of experimental data points. This optimisation problem is solved in a multi-start framework from different points in the parameter-space to obtain a high-quality solution. Parameter estimation was performed using the state-of-the-art interior point nonlinear optimisation solver IPOPT. The implementation in this work was programmed in the Python optimisation environment Pyomo [37]. Kinetic model simulation was conducted in the commercial software Mathematica™ 11.0.

RESULTS & DISCUSSION

Effects of light intensity and temperature on biomass growth

Both biomass growth rates and total biomass concentration increased with increasing incident light intensity from 20 μE to 60 μE, with a maximum at 100 μE, beyond which a decrease was observed (Fig. 1a). This indicates that photoinhibition becomes severe when light intensity reaches 300 μE, and optimal light intensity for cell growth may fall within the range between 100 μE to 300 μE. However, it should be noted that as a result of light attenuation, caused by light absorption and cell shading, incident and local light intensities within a PBR can be substantially different [28,34,38]. Thus, the optimal light intensity for the current mutant will be estimated further by the kinetic model.

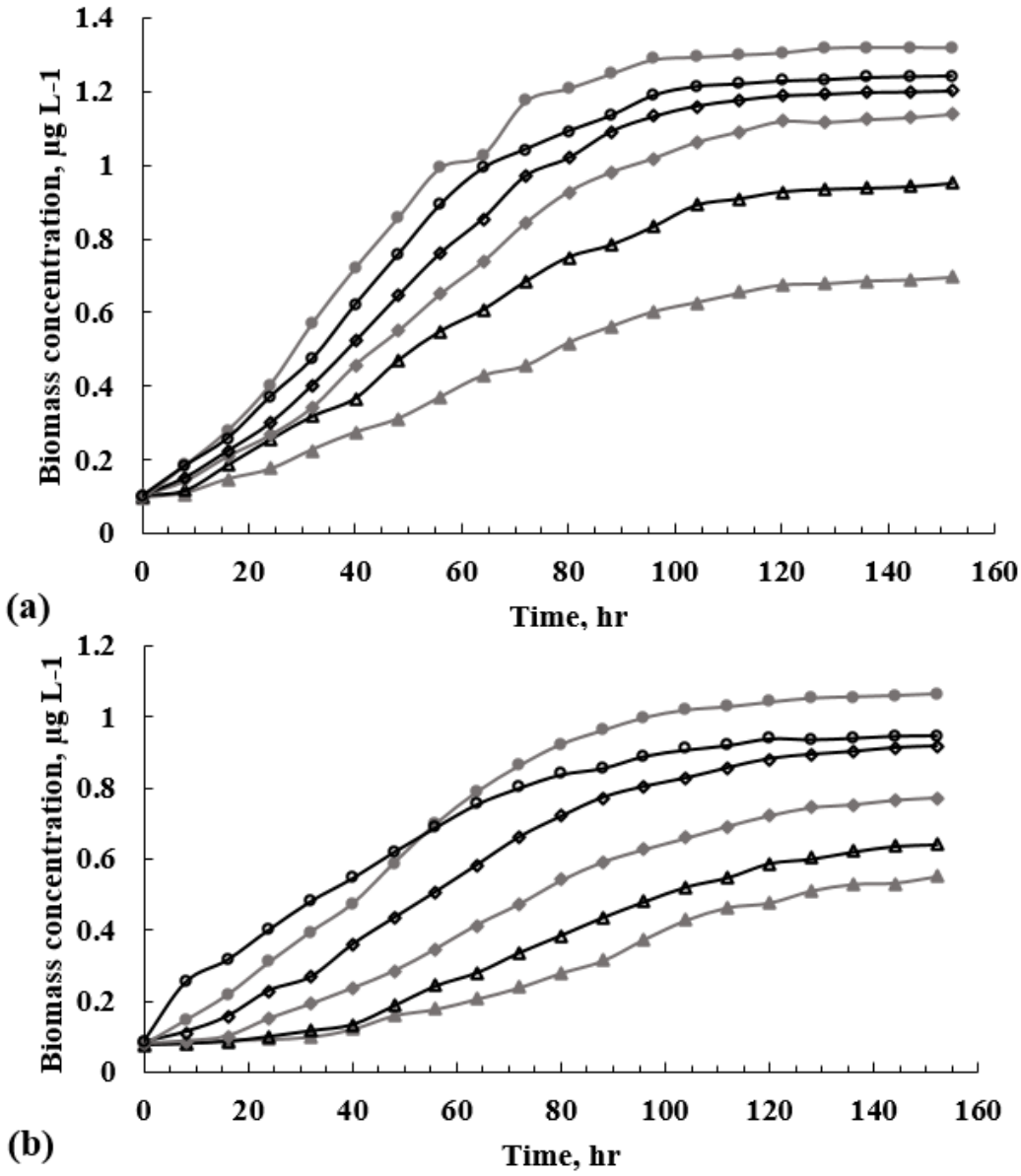

238

239 Figure 1: Growth of *C. reinhardtii* bisabolene production strain under different operating

240 conditions. (a): biomass growth at 30 ºC with incident light intensities of 20 µE (grey triangles),

241 40 µE (open triangles), 60 µE (grey diamonds), 80 µE (open diamonds), 100 µE (grey circles)

242 and 300 µE (open circles); (b): biomass growth with light intensity of 60 µE at temperatures of

243 22 ºC (grey triangles), 24 ºC (open triangles), 26 ºC (grey diamonds), 28 ºC (open diamonds),

244 30 ºC (grey circles) and 32 ºC (open circles).

The biomass growth rate was also found to be enhanced when the cultivation temperature was increased from 22 ºC to 30 ºC, beyond which a decrease in biomass growth rate and final biomass concentration was observed (Fig. 1b). In addition, the close match of the final biomass concentrations at 28 ºC and 32 ºC suggests that the culture temperature should be controlled within this range. Indeed, the optimal cultivation temperature for *C. reinhardtii* is known to fall within this range [39].

Effects of light intensity and temperature on bisabolene yields

Bisabolene concentrations were found to increase even after the culture reached stationary phase (~100 hours), regardless of the light intensity or temperature (Fig. 2). This indicates that bisabolene is synthesised from this strain at different growth phases and is not solely dependent on cell growth. It can also be seen that similar to biomass growth, bisabolene production reached a maximum at 100 µE (Fig. 2a) and 30 ºC (Fig. 2b), respectively. Bisabolene production followed similar trends with respect to cell accumulation and effects of temperature and light are almost identical compared to those on cell growth.

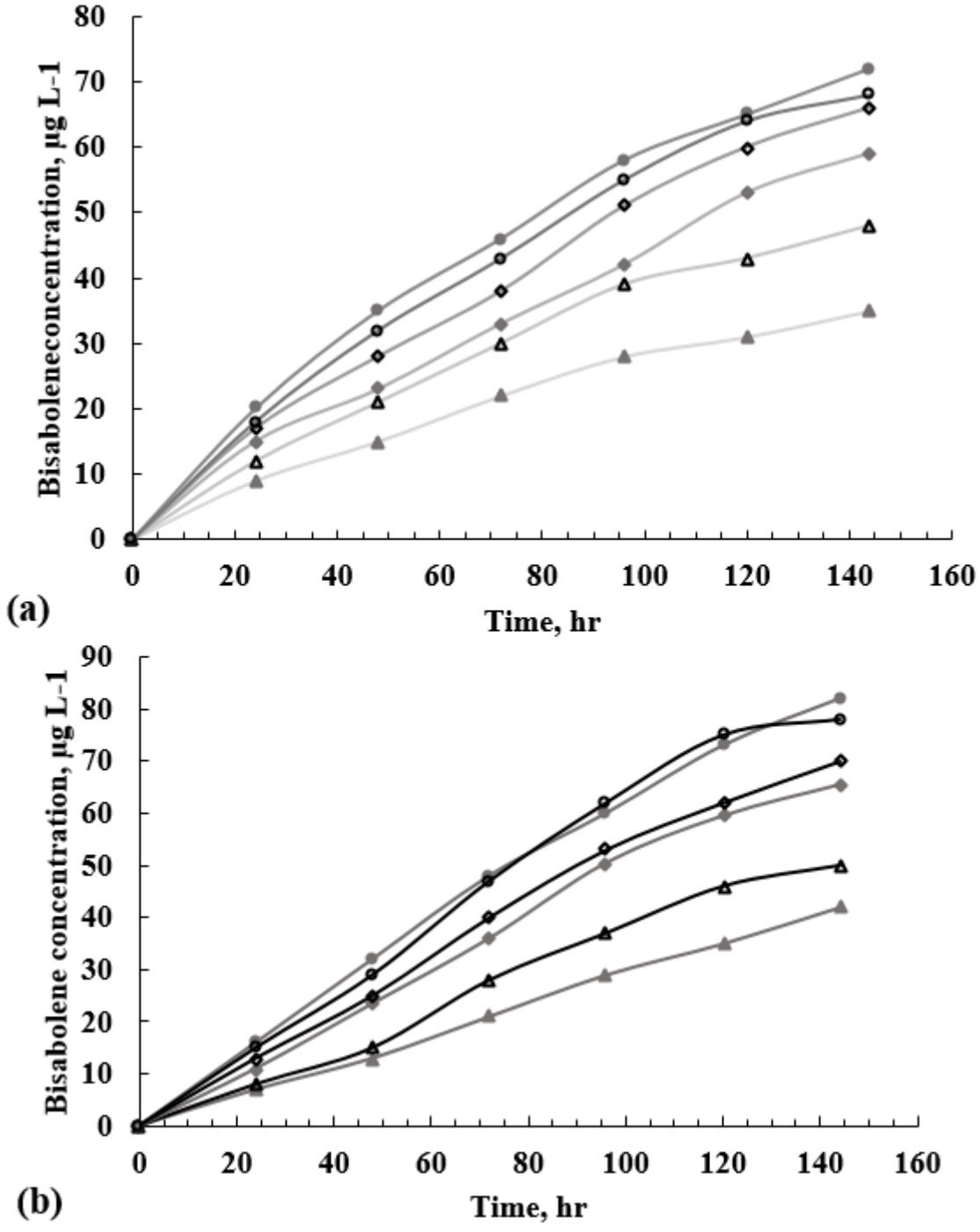

Figure 2: Bisabolene yields under different operating conditions. (a): bisabolene yields at 30 ºC with incident light intensities of 20 µE (grey triangles), 40 µE (open triangles), 60 µE (grey diamonds), 80 µE (open diamonds), 100 µE (grey circles) and 300 µE (open circles); (b): bisabolene yields with light intensity of 60 µE at temperatures of 22 ºC (grey triangles), 24 ºC

(open triangles), 26 ºC (grey diamonds), 28 ºC (open diamonds), 30 ºC (grey circles) and 32 ºC (open circles).

The above observations do not, however, imply that the optimal conditions for algal biomass growth and bisabolene synthesis are the same. Total volumetric bisabolene production (µg L^{-1}) is the product of biomass concentration (g L^{-1}) and the biomass-specific bisabolene productivity (µg g^{-1}). As a result, the total volumetric production of bisabolene can be increased at conditions favouring biomass growth, even if the biomass-specific bisabolene productivity is below optimal. Inefficient bisabolene production per biomass reduces the carbon and energy utilisation efficiency for bisabolene production, as well as increasing the consumption of nitrogen, phosphorus and minerals for undesired biomass production. Hence, effects of light intensity and temperature on bisabolene synthesis were further explored.

The comparison of the specific bisabolene productivities (µg g^{-1}) at the different light intensities shows little variation across the entire measurement range, suggesting that bisabolene synthesis is not directly linked to the change of light intensity (Table 2 and Fig. 3(a)). It was previously determined that day-night cycles could result in increased volumetric bisabolene productivities [21]. However, this effect was determined to be due to a prolonged exponential phase, rather than a difference at a cellular level, and supports the current finding that light intensity is not coupled to increases in the biomass-specific bisabolene productivity. Moreover, although the sesquiterpenoid pathway uses the same precursors as pigment biosynthesis, it is not directly coupled to photosynthesis. The precursor for bisabolene production, farnesyl pyrophosphate (FPP), is found in the cytoplasm rather than the chloroplast

and is used for sterol biosynthesis, rather than light harvesting, further supporting this finding [14,21].

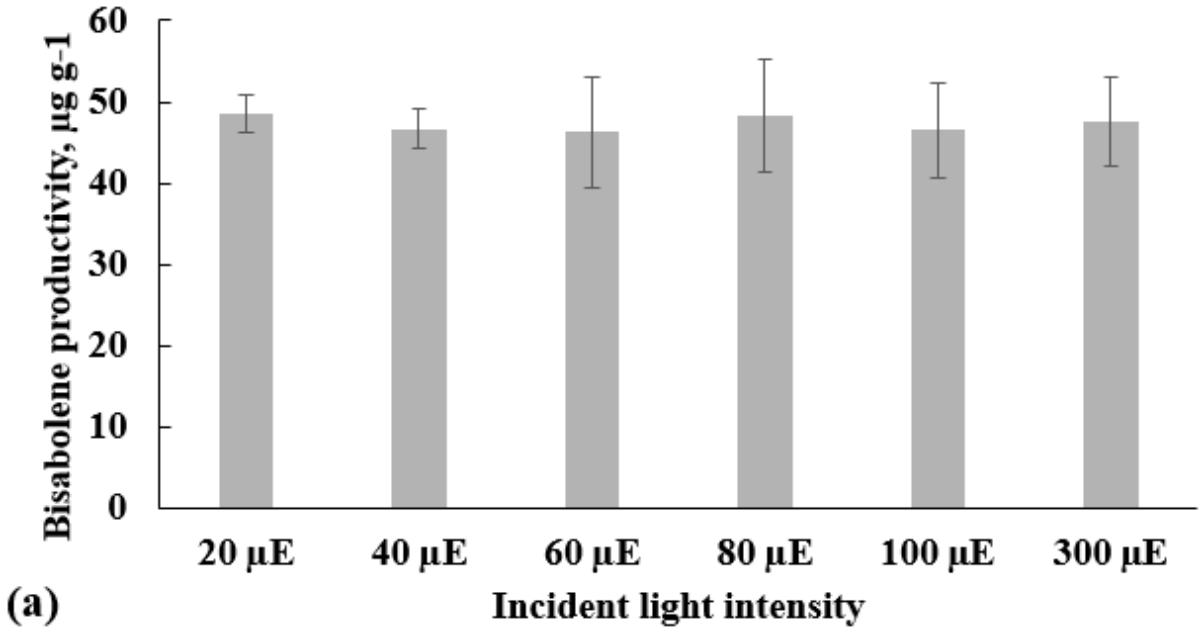

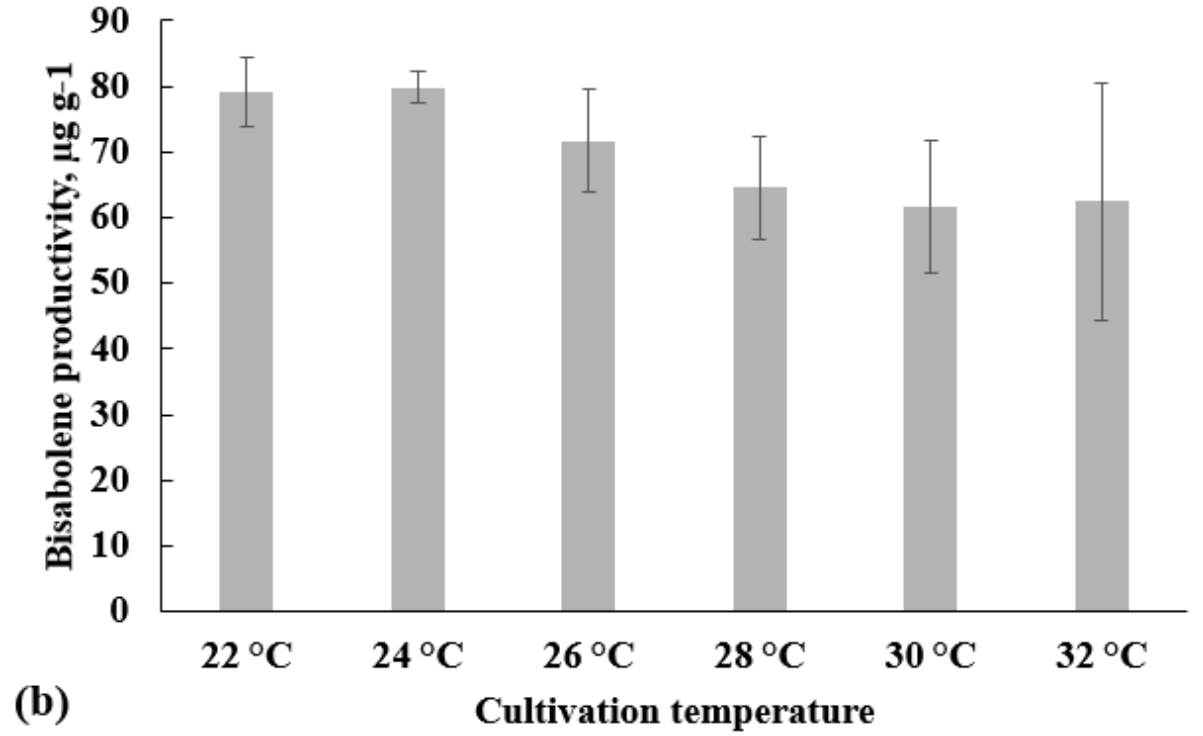

Figure 3: Biomass-specific, averaged bisabolene production under different operating conditions. (a): Effect of incident light intensity at 30 ºC; (b): Effect of cultivation temperature at 60 µE.

Table 2: Biomass-specific, averaged bisabolene production (μg g^{-1}_{DBM}) under different operating conditions

Different light intensity (μE), temperature fixed at 30 ºC.						
Light	20	40	60	80	100	300
Productivity	48.5 ± 2.3	46.7 ± 2.5	46.3 ± 6.7	48.3 ± 7.0	46.5 ± 5.9	47.6 ± 5.4
Different temperature (ºC), light intensity fixed at 60 μE						
Temperature	22	24	26	28	30	32
Productivity	79.1± 5.3	79.9± 2.3	71.7 ± 7.8	64.7 ± 7.8	61.5 ± 10.0	62.4 ± 18.0

It should be noted, however, that the current set of experiments was conducted under mixotrophic conditions with acetate in the growth medium. In mixotrophic conditions both mitochondrial respiration and photosynthesis act synergistically to increase culture growth rates. Indeed, in a previous study with the same host strain engineered to produce patchoulol, biomass and patchoulol yields were enhanced by the addition of acetate, although patchoulol production continued to increase even after the acetate had been depleted [14]. As sesquiterpene metabolism (bisabolene) is related to mitochondiral respiration rather than light harvesting, even in the absence of acetate, light intensity is unlikely to have any effect on the biomass-specific bisabolene productivities. This is different to the production of algal biohydrogen and biolipid, which are known to be limited by light related metabolic reactions associated with the photosynthetic electron transport chain [40,41].

In contrast to the effect of incident light, cellular bisabolene production is significantly affected by the culture temperature from 22 ºC to 30 ºC (Table 2 and Fig. 3(b)), particularly during the

306 early growth stage. A remarkable increase of 23.0% (from 61.5 μg g^{-1} to 79.9 μg g^{-1}) was
307 observed when the temperature decreased from 30 ºC to 24 ºC. This clearly indicates that the
308 optimal temperature for bisabolene synthesis is different from that for algal biomass growth,
309 and to maximise the bisabolene synthesis rate the cultivation temperature should be maintained
310 below 28 ºC. In addition, it can be concluded that the trend of cellular bisabolene production
311 with respect to temperature, *i.e.* decreasing from 24 ºC to 30 ºC, is exactly opposite to that of
312 cell growth. In fact, it is the reduction in cell growth which may directly contribute to increasing
313 the specific bisabolene productivity by prolonging the growth phases (Fig. 1(b)). A similar
314 effect was observed when cultivating the strain under light-dark cycles, which as expected
315 slowed down growth, final bisabolene titres were increased by up to 50%.
316 Interestingly, the calculated bisabolene productivities for the low temperature experiments
317 were much more consistent over the whole growth cycle than the higher temperature
318 experiments, which are significantly reduced in the growth phases and only recovered in the
319 stationary phase. Indeed, the application of a dodecane overlay for the *in-situ* recovery of
320 bisabolene increased the overall product yield more than five-fold compared to cultivation
321 without dodecane [21]. Consequently, further studies should be conducted to test the online
322 recovery of bisabolene, to investigate whether overall productivities could be increased. In all
323 cases, to maximise the solar conversion efficiency towards bisabolene and maintain high
324 biofuel production rates, it is vital to identify operating conditions under which the culture
325 volumetric bisabolene productivity is maintained high. As a result, an accurate dynamic model

capable of simulating both algal biomass growth and bisabolene production becomes an efficient tool to resolve this challenge.

Results of kinetic model construction

The current parameter estimation results are listed in Table 3. From the table, it is seen that bubble scattering coefficient was estimated to be 0, suggesting its effect on light transmission is negligible compared to cell absorption (Table 3). Comparing the model results to the experimental data shows that the current model provides a good representation of the dynamic trend of both biomass growth and bisabolene production (Fig. 4). Except of a slight underestimation of biomass concentration at the beginning period of Experiment 4, the model maximum fitting error is 13.9% occurring at the 96th hour for bisabolene production in Experiment 2, with an average fitting error around 5% for these four experiments.

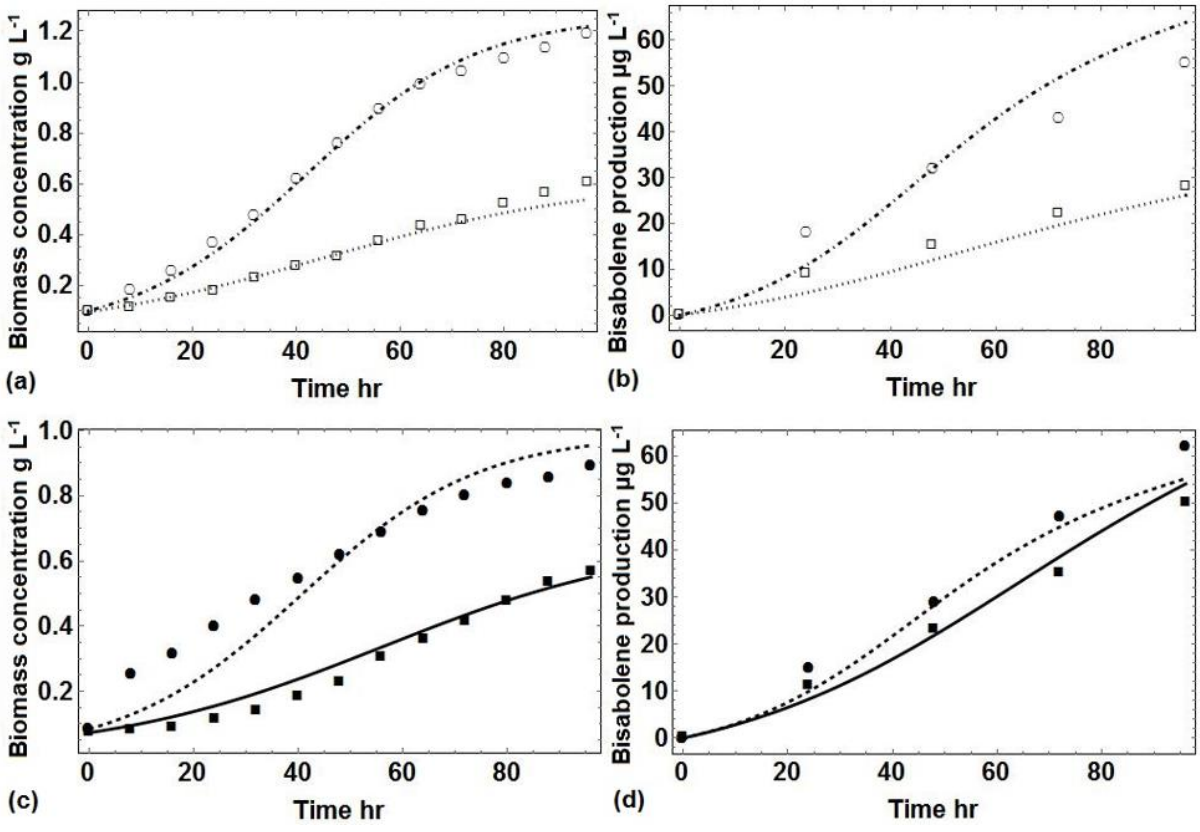

Figure 4: Dynamic model simulation results for biomass growth (a, c) and bisabolene production (b, d): Dotted line: model fitting results for Experiment 1 (open squares); Dot-dashed line: model fitting results for Experiment 2 (open circles); Thick line: model fitting results for Experiment 3 (filled squares); Dashed line: model fitting results for Experiment 4 (filled circles).

Table 3: Parameter estimation results for the current dynamic model

Parameter	Value	Parameter	Value
μ, h^{-1}	0.304	E_a, kJ mol^{-1}	144.0
μ_d, L g^{-1} h^{-1}	5.075×10^{-2}	E_b, kJ mol^{-1}	343.9
k_s, µE	34.92	T_a, K	306.7
k_i, µE	441.2	T_b, K	307.1
τ, L g^{-1} m^{-1}	0.0339	Y_1, µg g^{-1}	326.7
K_a, m^{-1}	0.0	Y_2, µg g^{-1} h^{-1}	1.758
α, --	0.474		

Dynamic model predictive capability

To facilitate the process design, optimisation, and control for future algal biosabolene production, it is essential that the model is capable of accurately predicting the dynamic performance of an unknown process. Therefore, the predictive capability of the current model was verified against the four test experiments executed under different operating conditions (Fig. 5). In most cases, the error was less than 5%, with a maximum error of 20.3%, at the 96th hour for biomass concentration in Test 4, suggesting that the model effectively predicts

biomass growth and bisabolene production throughout the experiments even at the most severe conditions (*e.g.* Test 4 where temperature was the lowest). Hence, the model has great predictive capability and can be used for further process optimisation and control.

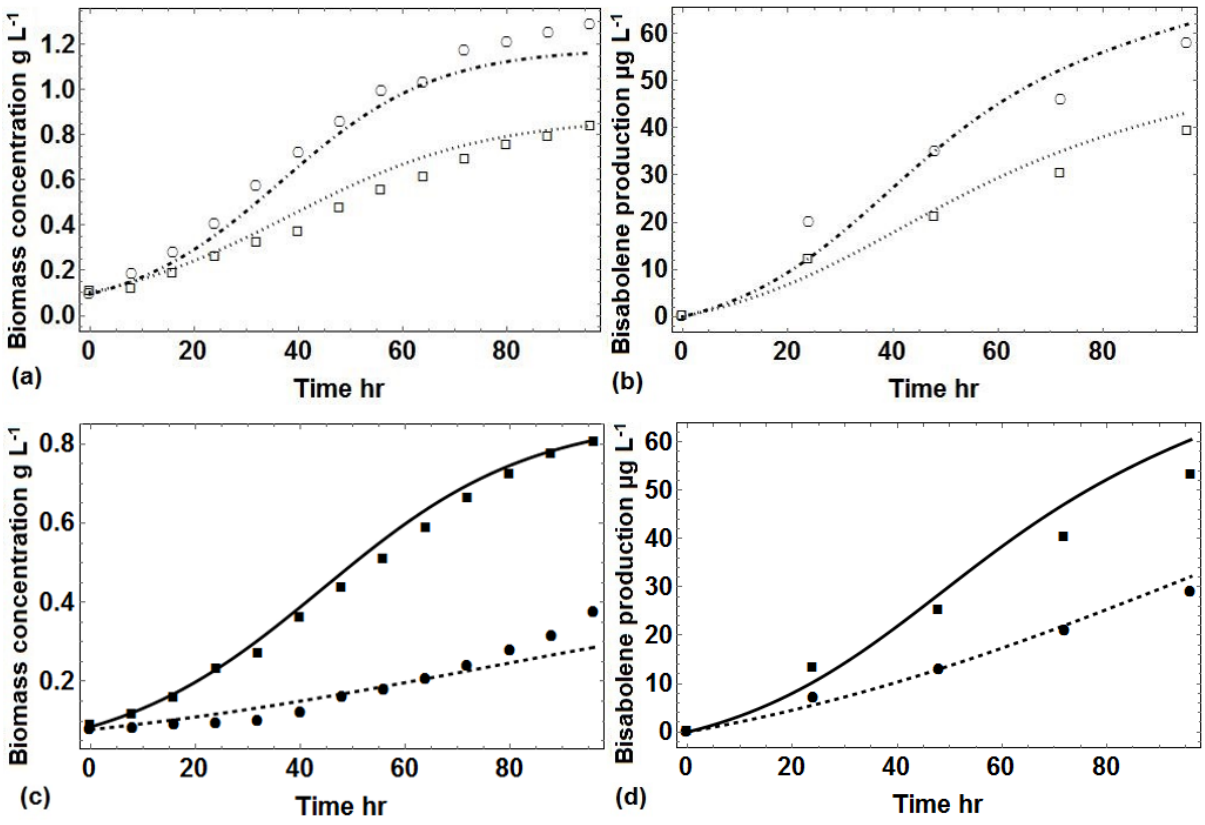

Figure 5: Dynamic model prediction results for biomass growth (a, c) and bisabolene production (b, d): Dotted line: model prediction results for Test 1 (open squares); Dot-dashed line: model prediction results for Test 2 (open circles); Thick line: model prediction results for Test 3 (filled squares); Dashed line: model prediction results for Test 4 (filled circles).

Impact of light attenuation on mutant growth

Based on the model, the impact of light attenuation on biomass growth was analysed (Table 4). It was found that unlike previous results for cyanobacteria cultures [28], the effect of microalgal cell absorption on local light intensities within the PBR was relatively low. Even at the maximum algal biomass concentrations achieved in this study (1.3 g L^{-1}), the average light

intensity in the PBR was 60.6% of the incident light intensity, whilst the lowest local light intensity at the reactor front surface remained at 32.7% of the incident light intensity. This conclusion is consistent with the recent study in which a thorough comparison on light attenuation induced by different species, in particular green alga *C. reinhardtii* and cyanobacterium *Cyanothece* sp., was presented [42]. The study declared that compared to cyanobacteria, cell absorption caused by green algae is much milder in a laboratory scale PBR, and may not be the primary limiting factor for cell growth and biorenewables synthesis until the very end of the experiment.

Table 4: Average light intensity (% incident light intensity) at different biomass concentration

Algal biomass concentration	Lab-scale (width 0.025 m)	Pilot scale (width 0.25 m)
0.1 g L^{-1}	95.9%	67.5%
0.5 g L^{-1}	81.5%	23.3%
0.9 g L^{-1}	70.0%	13.1%
1.3 g L^{-1}	60.6%	9.1%

However, once the reactor is scaled up into a pilot system, and the width of the flat-plate PBR is increased from 0.025 m to 0.25 m, the current simulation results show that the average light intensity in the reactor decreases dramatically. For instance, at a cell concentration of 0.5 g L^{-1} average light intensity decreases by 76.7% compared to the incident light intensity (Table 4), and local light intensities at the reactor front drops to zero based on the current calculation if illumination is provided only from the back. This indicates that once the system is scaled up,

the primary challenge for biomass growth and bioproducts synthesis may switch from intrinsic limits (*e.g.* metabolic activities) to process scale-up issues (*e.g.* reactor design).

Optimal light intensity and temperature

Finally, as the effect of light attenuation was minor in the current experiments, optimal light intensity for the mutant growth should be close to the measured optimum (100 μE). By taking into account light attention, optimal light intensity and temperature for algal cell growth were estimated to be 124.2 μE and 30.8 ºC, respectively. As the effect of light intensity on bisabolene synthesis was also found to be minor, optimal light intensity for bisabolene production could be fixed same as that for biomass growth. Nonetheless, to balance the temperature trade-off effect between cell growth and bisabolene synthesis, optimal temperature for total volumetric bisabolene production was estimated to be 30.9 ºC. The similarities in the optimal temperatures for biomass growth and total bisabolene production suggest that total bisabolene production is dominated by biomass concentration rather than high biomass-specific bisabolene productivity. As a result, a combination of 124.2 μE and 30.9 ºC can be considered as the optimal operating condition for continuous algal bisabolene production.

CONCLUSION

In this study, effects of light intensity and temperature on both the modified *Chlamydomonas reinhardtii* UVM4 biomass growth and bisabolene (excreted biofuel) synthesis were investigated. Through experimental analysis and dynamic modelling, the current research found that under mixotrophic growth conditions, bisabolene was partially expressed independent of biomass growth, resulting in continued production during the stationary phase.

Whilst light intensity had minimal effect on the biomass-specific bisabolene productivity, bisabolene formation was strongly favoured at low and high temperatures, at which biomass growth was reduced. Nevertheless, as the overall bisabolene production is proportional to the biomass concentration, the optimal temperature for bisabolene productivity deviates only slightly from that for biomass growth. It is therefore concluded that optimal conditions for cell growth and biofuel production are different, and robust bioprocess real-time optimisation strategies should be adopted to guarantee high resources conversion efficiency when scaling up this system. This research, therefore, paves the way for future studies of sustainable excreted algal biofuels and mutant development.

Acknowledgments

This project has received funding from the European Union's Horizon 2020 research and innovation programme under grant agreement No 640720. This project has also received funding from the EPSRC project (EP/P016650/1, P65332). Irina acknowledges funding from the Ministry of Higher Education, Malaysia and University Putra Malaysia. The bisabolene excreting mutant of *Chlamydomonas reinhardtii* was developed by Julian Wichmann and Kyle J. Lauersen working in the group of Olaf Kruse at Universität Bielefeld, Germany.

References

1. Radakovits R, Jinkerson RE, Darzins A, Posewitz MC. Genetic engineering of algae for enhanced biofuel production. *Eukaryot Cell*. 2010;9(4):486-501. doi:10.1128/EC.00364-09.

2. Parmar A, Singh NK, Pandey A, Gnansounou E, Madamwar D. Cyanobacteria and

microalgae: A positive prospect for biofuels. *Bioresour Technol*. 2011;102(22):10163-10172. doi:10.1016/j.biortech.2011.08.030.

3. Chisti Y. Constraints to commercialization of algal fuels. *J Biotechnol*. 2013;167(3):201-214. doi:10.1016/j.jbiotec.2013.07.020.

4. Rawat I, Ranjith Kumar R, Mutanda T, Bux F. Biodiesel from microalgae: A critical evaluation from laboratory to large scale production. *Appl Energy*. 2013;103(0):444-467. doi:10.1016/j.apenergy.2012.10.004.

5. Mikkonen S, Hartikka T, Kuronen M, Saikkonen P. *HVO, Hydrotreated Vegetable Oil - a Premium Renewable Biofuel for Diesel Engines*.; 2012.

6. Wagner J, Bransgrove R, Beacham TA, Allen M, Meixner K, Drosg B, Ting V, Chuck C. Co-production of bio-oil and propylene through the hydrothermal liquefaction of polyhydroxybutyrate producing cyanobacteria. *Bioresour Technol*. 2016;207:166-174. doi:10.1016/j.biortech.2016.01.114.

7. Wagner JL, Le CD, Ting VP, Chuck CJ. Design and operation of an inexpensive, laboratory-scale, continuous hydrothermal liquefaction reactor for the conversion of microalgae produced during wastewater treatment. *Fuel Process Technol*. 2017;165:102-111. doi:10.1016/j.fuproc.2017.05.006.

8. Tian C, Li B, Liu Z, Zhang Y, Lu H. Hydrothermal liquefaction for algal biorefinery: A critical review. *Renew Sustain Energy Rev*. 2014;38:933-950. doi:10.1016/j.rser.2014.07.030.

9. Kato A, Takatani N, Ikeda K, Maeda S, Omata T. Removal of the product from the

culture medium strongly enhances free fatty acid production by genetically engineered Synechococcus elongatus. *Biotechnol Biofuels*. 2017;10(1):141. doi:10.1186/s13068-017-0831-z.

10. Pade N, Mikkat S, Hagemann M. Ethanol, glycogen and glucosylglycerol represent competing carbon pools in ethanol-producing cells of Synechocystis sp. PCC 6803 under high-salt conditions. *Microbiology*. 2017;163(3):300-307. doi:10.1099/mic.0.000433.

11. Hirokawa Y, Dempo Y, Fukusaki E, Hanai T. Metabolic engineering for isopropanol production by an engineered cyanobacterium, Synechococcus elongatus PCC 7942, under photosynthetic conditions. *J Biosci Bioeng*. 2017;123(1):39-45. doi:10.1016/j.jbiosc.2016.07.005.

12. Halfmann C, Gu L, Gibbons W, Zhou R. Genetically engineering cyanobacteria to convert CO2, water, and light into the long-chain hydrocarbon farnesene. *Appl Microbiol Biotechnol*. 2014;98(23):9869-9877. doi:10.1007/s00253-014-6118-4.

13. del Rio-Chanona EA, Zhang D, Shah N. Sustainable biopolymer synthesis via superstructure and multiobjective optimization. *AIChE J*. July 2017. doi:10.1002/aic.15877.

14. Lauersen KJ, Baier T, Wichmann J, Wördenweber R, Mussgnug JH, Hübner W, Huser T, Kruse O. Efficient phototrophic production of a high-value sesquiterpenoid from the eukaryotic microalga Chlamydomonas reinhardtii. *Metab Eng*. 2016;38:331-343. doi:10.1016/j.ymben.2016.07.013.

15. Misawa N. Pathway engineering for functional isoprenoids. *Curr Opin Biotechnol*. 2011;22(5):627-633. doi:10.1016/j.copbio.2011.01.002.

16. Bohlmann J, Crock J, Jetter R, Croteau R. Terpenoid-based defenses in conifers: cDNA cloning, characterization, and functional expression of wound-inducible (E)- -bisabolene synthase from grand fir (Abies grandis). *Proc Natl Acad Sci*. 1998;95(12):6756-6761. doi:10.1073/pnas.95.12.6756.

17. Peralta-Yahya PP, Ouellet M, Chan R, Mukhopadhyay A, Keasling JD, Lee TS. Identification and microbial production of a terpene-based advanced biofuel. *Nat Commun*. 2011;2:483. doi:10.1038/ncomms1494.

18. Baba M, Shiraiwa Y. Biosynthesis of lipids and hydrocarbons in algae. In: Dubinsky Z, ed. *Photosynthesis*. ; 2013:321-355. doi:10.5772/56413.

19. Melis A. Carbon partitioning in photosynthesis. *Curr Opin Chem Biol*. 2013;17(3):453-456. doi:10.1016/j.cbpa.2013.03.010.

20. Davies FK, Work VH, Beliaev AS, Posewitz MC. Engineering Limonene and Bisabolene Production in Wild Type and a Glycogen-Deficient Mutant of Synechococcus sp. PCC 7002. *Front Bioeng Biotechnol*. 2014;2. doi:10.3389/fbioe.2014.00021.

21. Wichmann J, Baier T, Wentnagel E, Lauersen KJ, Kruse O. Tailored carbon partitioning for phototrophic production of (E)-α-bisabolene from the green microalga Chlamydomonas reinhardtii. *Metab Eng*. 2018;45:211-222. doi:10.1016/j.ymben.2017.12.010.

22. Scaife MA, Nguyen GTDT, Rico J, Lambert D, Helliwell KE, Smith AG. Establishing Chlamydomonas reinhardtii as an industrial biotechnology host. *Plant J.* 2015;82(3):532-546. doi:10.1111/tpj.12781.

23. Neupert J, Karcher D, Bock R. Generation of Chlamydomonas strains that efficiently express nuclear transgenes. *Plant J.* 2009;57(6):1140-1150. doi:10.1111/j.1365-313X.2008.03746.x.

24. Gorman DS, Levine RP. Photosynthetic Electron Transport Chain of Chlamydomonas reinhardi . V . Purification and Properties of Cytochrome 553 and Ferredoxin. *Plant Physiol*. 1966;41(0):1643-1647.

25. Tamburic B, Zemichael FW, Crudge P, Maitland G, Hellgardt K. Design of a novel flat-plate photobioreactor system for green algal hydrogen production. *Int J Hydrogen Energy*. 2011;36(11):6578-6591. doi:10.1016/j.ijhydene.2011.02.091.

26. Jing K, Tang Y, Yao C, del Rio-Chanona EA, Ling X, Zhang D. Overproduction of L-tryptophan via simultaneous feed of glucose and anthranilic acid from recombinant E.coli W3110: kinetic modelling and process scale-up. *Biotechnol Bioeng*. August 2017. doi:10.1002/bit.26398.

27. Dechatiwongse P, Srisamai S, Maitland G, Hellgardt K. Effects of light and temperature on the photoautotrophic growth and photoinhibition of nitrogen-fixing cyanobacterium Cyanothece sp. ATCC 51142. *Algal Res*. 2014;5(0):103-111. doi:10.1016/j.algal.2014.06.004.

28. Zhang D, Dechatiwongse P, del Rio-Chanona E a., Maitland GC, Hellgardt K,

505 Vassiliadis VS. Modelling of light and temperature influences on cyanobacterial growth
506 and biohydrogen production. *Algal Res*. 2015;9:263-274.
507 doi:10.1016/j.algal.2015.03.015.
508 29. Béchet Q, Shilton A, Guieysse B. Modeling the effects of light and temperature on algae
509 growth: State of the art and critical assessment for productivity prediction during
510 outdoor cultivation. *Biotechnol Adv*. 2013;31(8):1648-1663.
511 doi:10.1016/j.biotechadv.2013.08.014.
512 30. del Rio-Chanona EA, Ahmed N rashid, Zhang D, Lu Y, Jing K. Kinetic modeling and
513 process analysis for Desmodesmus sp. lutein photo-production. *AIChE J*.
514 2017;63(7):2546-2554. doi:10.1002/aic.15667.
515 31. Mu Y, Yang H-Y, Wang Y-Z, He C-S, Zhao Q-B, Wang Y, Yu H-Q. The maximum
516 specific hydrogen-producing activity of anaerobic mixed cultures: definition and
517 determination. *Sci Rep*. 2015;4(1):5239. doi:10.1038/srep05239.
518 32. Río E Del, Acién FG, García-Malea MC, Rivas J, Molina-Grima E, Guerrero MG.
519 Efficient one-step production of astaxanthin by the microalgaHaematococcus pluvialis
520 in continuous culture. *Biotechnol Bioeng*. 2005;91(7):808-815. doi:10.1002/bit.20547.
521 33. Dechatiwongse P, Maitland G, Hellgardt K. Demonstration of a two-stage
522 aerobic/anaerobic chemostat for the enhanced production of hydrogen and biomass from
523 unicellular nitrogen-fixing cyanobacterium. *Algal Res*. 2015;10:189-201.
524 doi:10.1016/j.algal.2015.05.004.
525 34. del Rio-Chanona EA, Zhang D, Xie Y, Manirafasha E, Jing K. Dynamic Simulation and

526 Optimization for Arthrospira platensis Growth and C-Phycocyanin Production. *Ind Eng*
527 *Chem Res*. 2015;54(43):10606-10614. doi:10.1021/acs.iecr.5b03102.
528 35. Kameswaran S, Biegler LT. Convergence rates for direct transcription of optimal control
529 problems using collocation at Radau points. *Comput Optim Appl*. 2008;41(1):81-126.
530 doi:10.1007/s10589-007-9098-9.
531 36. Faber R, Li P, Wozny G. Sequential Parameter Estimation for Large-Scale Systems with
532 Multiple Data Sets. 1. Computational Framework. *Ind Eng Chem Res*.
533 2003;42(23):5850-5860. doi:10.1021/ie030296s.
534 37. del Rio-Chanona EA, Dechatiwongse P, Zhang D, Maitland G, Hellgardt K, Arellano-
535 Garcia H, Vassiliadis V. Optimal Operation Strategy for Biohydrogen Production. *Ind*
536 *Eng Chem Res*. 2015;54(24):6334-6343. doi:10.1021/acs.iecr.5b00612.
537 38. Zhang D, Wan M, del Rio-Chanona EA, Huang J, Wang W, Li Y, Vassiliadis V.
538 Dynamic modelling of Haematococcus pluvialis photoinduction for astaxanthin
539 production in both attached and suspended photobioreactors. *Algal Res*. 2016;13:69-78.
540 doi:10.1016/j.algal.2015.11.019.
541 39. Copyright. In: *The Chlamydomonas Sourcebook*. Elsevier; 2009:iii. doi:10.1016/B978-
542 0-12-370873-1.00059-9.
543 40. Johnson X, Alric J. Central Carbon Metabolism and Electron Transport in
544 Chlamydomonas reinhardtii: Metabolic Constraints for Carbon Partitioning between Oil
545 and Starch. *Eukaryot Cell*. 2013;12(6):776-793. doi:10.1128/EC.00318-12.
546 41. Cardol P, Forti G, Finazzi G. Regulation of electron transport in microalgae. *Biochim*

Biophys Acta - Bioenerg. 2011;1807(8):912-918. doi:10.1016/j.bbabio.2010.12.004.

42. Zhang D, Chanona EAD-R, Vassiliadis VS, Tamburic B. Analysis of green algal growth via dynamic model simulation and process optimization. *Biotechnol Bioeng*. 2015;112(10). doi:10.1002/bit.25610.

Table of Contents